RSC Advances

PAPER

View Article Online
View Journal | View Issue



Cite this: *RSC Adv.*, 2020, **10**, 44512

# Novel ammonium dichloroacetates with enhanced herbicidal activity for weed control†

Huanhuan Li,[a] Yajie Ma,[a] Hongyan Hu,[a] Xianpeng Song,[a] Yan Ma*[a] and Hong Yan*[b]

Received 13th October 2020
Accepted 23rd November 2020

DOI: 10.1039/d0ra08707f

rsc.li/rsc-advances

Dichloroacetic acid (DCA) exhibits great potential as an herbicide (nontoxic, easily biodegradable), but its application in agriculture has scarcely been investigated. Since DCA readily undergoes photolysis when exposed to natural light or UV irradiation, there is a large activity loss in controlling weeds. To improve the activity of DCA, we proposed the transformation of DCA into an ionic salt form by using an herbicidal ionic liquids (HILs) strategy. Herein, fifteen novel ammonium dichloroacetates were designed and achieved for the first time. When compared to the anionic precursor DCA, three salts with longer alkyl chains ranging from dodecyl to hexadecyl chains were found to enhance not only the post emergence herbicidal activity but also the rates of activity against some broadleaf weeds under greenhouse conditions. The enhancement was due to the synergistic effect of structural factors, such as the surface activity, solubility and stability arising from their ionic nature. In addition, IL 13 possesses a low phytotoxicity to cotton plants with a favorable selectivity index above 2. This study will be useful for the design of new, high-performance herbicidal formulations.



## 1 Introduction

Weeds are an important biodisaster class in agriculture. They intensely compete with crops for light, water and nutrients, and also host crop pests, bacteria and fungi, therefore cause a greater reduction in both the quantity and quality of crop production.[1] Currently, chemical herbicides remain the most effective way to control weeds in agricultural practices.[2] However, some failed to control weeds during application because of issues with, volatility,[3] solubility[4] or stability,[5] that even adversely affect the bio-efficacy and agro-ecological security.[6]

To address these issues, herbicidal ionic liquids (HILs) strategy can be employed early in 2011,[7] in which the herbicides are developed into new IL forms. Such HILs are ionic salts with melting point below 100 °C, usually composed of active herbicidal anions and cations. These polar HILs are very soluble in water, not volatile, and thermally/chemically stable. These properties make them have enhanced performance, better biodegradability and lower toxicity than its model anionic herbicides.[7–24] For instance, Cojocaru *et al.* synthesized dicamba HILs to avoid high volatile drift problems of dicamba acid, and found that dicamba tetrabutylammonium salt reduced volatility with a 0.7% volatilization loss *versus* a 10.8% loss of dicamba acid after 12 h isotherms at 75 °C.[8] This can minimize the risk of off-site movement to humans, non-target organisms and other agricultural ecosystems *via* volatilization. Pernak *et al.* prepared glyphosate HILs to solve the poor solubility of glyphosate acid (only 1.2–1.4% soluble in water),[4] among which, di(bis(2-hydroxyethyl)-cocomethylammonium) glyphosate was shown to improve the herbicidal efficacy by increasing the water solubility by 2.5–3 times, much higher than the commercial formulation Roundup 360 SL, and it would lower the dose of glyphosate by more than 50%.[9] Niemczak *et al.* changed auxin herbicides (*i.e.*, 2,4-D, MCPA) in to their ammonium salt, and effectively reduced toxicity (acute oral $LD_{50}$ 300–2000 mg $kg^{-1}$ for rats) and enhanced biodegradability (≥62% degradation after 28 days in an OECD 301F Test).[10] Similar results had also been observed in the other HILs based on clopyralid,[11] bentazone,[12] picloram,[13] 2,2′-thiodiacetic acid,[14] *etc*,[15–24] which were incorporated with special cations. Notably, not every HIL was safe, and some HILs were still shown to influence soil microorganism (*Proteobacteria*, *Chlamydiae* or *Bacteroidetes*).[25] Although HILs have both advantages and disadvantages, but the use of HILs in agricultural applications is well accepted.

Dichloroacetic acid (DCA) and its sodium or diisopropylammonium salt, pyruvate dehydrogenase kinase (PDK)

[a]*Plant Protection Department, State Key Laboratory of Cotton Biology, Institute of Cotton Research, The Chinese Academy of Agricultural Sciences, Henan, Anyang 455000, China. E-mail: aymayan@126.com; Fax: +86-372-2562294; Tel: +86-372-2562294*

[b]*State Key Laboratory of Coordination Chemistry, School of Chemistry and Chemical Engineering, Nanjing University, Nanjing, Jiangsu 210023, P. R. China. E-mail: hyan1965@nju.edu.cn*

† Electronic supplementary information (ESI) available: $^{1}H$ and $^{13}C$ NMR spectra, solubility and surface tension results, preliminary screening of herbicidal activity, the image of the response of some broadleaf weeds after treatments. See DOI: 10.1039/d0ra08707f

inhibitors, have been well known to possess diverse pharmacologic properties, *e.g.*, antitumor,[26] anticancer,[27] antimetabolic agents,[28] therapeutic agents,[29] oral antidiabetic agents,[30] and more. However, the phytotoxicity of DCA to weed plants has been barely investigated. Early in the mid-1980s, DCA was found to have phytotoxicity, where it can inhibit electron transport between menaquinone $Q_A$ and ubiquinone $Q_B$ at the reductase side in plant photosystem II (PSII) reaction centers.[31] Being a potential herbicide, DCA has a short persistence (21 days) in water and soil due to its easy biodegradation *via* microbial dehalogenases, and has little impact on subsequent rotated crops.[32] However, if exposed to natural light or UV irradiation, DCA is vulnerable to being dechlorinated and decomposing to inactive products, such as hydrochloric acid and carbon dioxide,[33] which therefore largely affect its activity in controlling weeds.

As the "HIL" strategy implied, the transformation of DCA into a stable ionic salt form might improve its activity. DCA, a strong acid ($pK_a = 1.29$), can be fully deprotonated as the dichlorocetate anion to generate salts with ammonium cations. Herein, we designed a novel and active class of ammonium dichloroacetates ILs containing cations with biogenic 2-hydroxyethylamine[34] and a fixed phytotoxic dichlorocetate anion (Scheme 1) and demonstrate their abilities to enhance herbicidal activity against weeds compared to that of the DCA control.

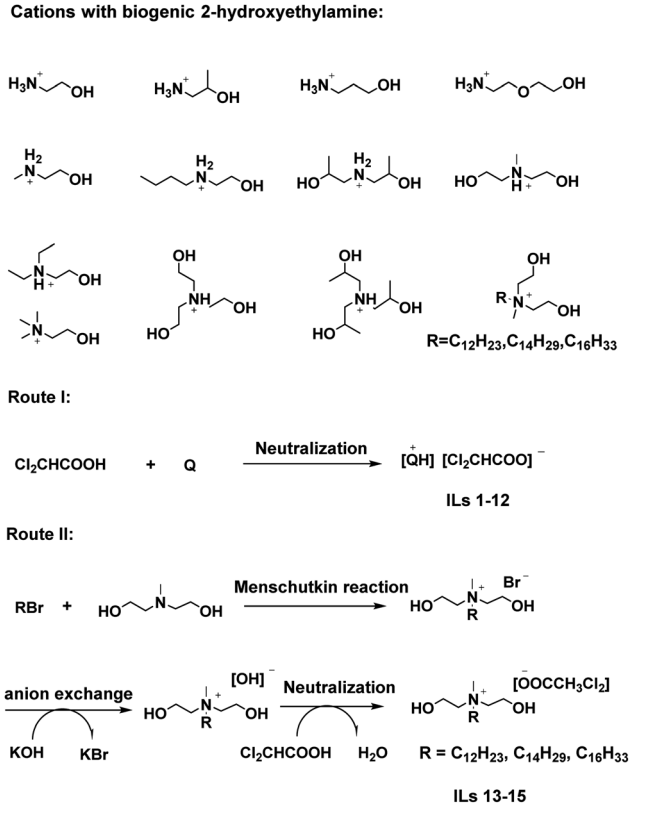


Scheme 1 Structures of ammonium cations used and the synthetic routes of ammonium dichloroacetates ILs.

## 2 Results and discussion

### 2.1 Synthesis and characterization of ILs

Fifteen ammonium dichloroacetates were first synthesized through acid–base neutralization but in two different routes (Scheme 1). In the first, DCA was directly neutralized with primary (1°), secondary (2°) and tertiary (3°) hydroxylalkylamines in a 1.1 : 1.0 mole ratio to form ILs 1–12. In the second, 1-bromoalkanes with different linear alkyl chains ($C_{12}$, $C_{14}$ or $C_{16}$) were converted to quaternary alkylammonium bromide by the Menschutkin reaction with *N*-methyldiethanolamine, followed by an anion-exchange with hydroxide and neutralization with DCA to yield ILs 13–15. The final salts were purified by extraction of DCA with excess diethyl ether and isolated by evaporation in yields of over 90%. The above synthetic strategy could provide an economic, efficient and easy-to-operate approach for producing ammonium dichloroacetates on a large scale. It should be stressed that the second method trough acid–base reactions of ammonium hydroxides and DCA, not metathesis of ammonium hydroxides halides with sodium salts of DCA, proved to be efficient at minimizing the separation difficulties of KBr. Moreover, this method has been used in the preparation of HILs based on dicamba acid or glyphosate acid.[8,9]

NMR analysis confirmed the formation of salts (Fig. S1–S30, ESI†). In the $^1$H NMR spectra (in DMSO-$d_6$), the acidic proton of DCA at 12.48 ppm completely disappeared, and new characteristic signals of protonated 1°–3° ammonium cations in ILs 1–9 were observed as a broad singlet at 5.65–9.98 ppm. In the $^{13}$C NMR spectra, the chemical signal assigned to the carboxyl of the dichlorocetate anion appeared at approximately 165 ppm. The results demonstrated that the proton was successfully transferred from DCA to the amines, which implied that the newly prepared ILs were ionic salts rather than either the mixture of acid and base or amides.

These salts were isolated as either a viscous liquid or a low melting point solid with the melting points below 100 °C, and hence were classified as ionic liquids, with one exception where IL 2 had a higher melting point above 100 °C. They were all nonvolatile, soluble in polar organic solvents, *i.e.*, water, methanol, dimethylsulfoxide, acetonitrile, acetone, and isopropanol, and insoluble in toluene or diethyl ether except ILs 13–15, which were partially soluble (Table S1, ESI†). Good water solubility is vital to increasing the uptake of ILs by plants through preventing crystallization, slowing drying and prolonging spray retention in liquid for absorption,[35] which further improve the ultimate herbicidal activity.

### 2.2 Surface activity

The surface tension of aqueous solutions of ILs was measured by the platinum ring method at 298 K. All ILs reduced the surface tension of aqueous solutions (Fig. 1 and S31†). Particularly, only three salts, ILs 13–15, were found to self-assemble into micelles (Fig. 1). This was related to the chemical structure. Due to both the long hydrophobic alkyl chains, and hydrophilic 4° ammonium and hydroxylethyl groups were

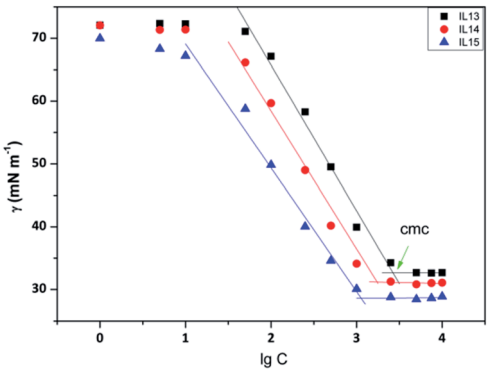


Fig. 1 Surface tension ($\gamma$[mN $m^{-1}$]) data *vs.* the logarithm of concentration (C mg $L^{-1}$) isotherms measured at 298 K for aqueous solutions of ILs 13–15. The position of the cmc is indicated.

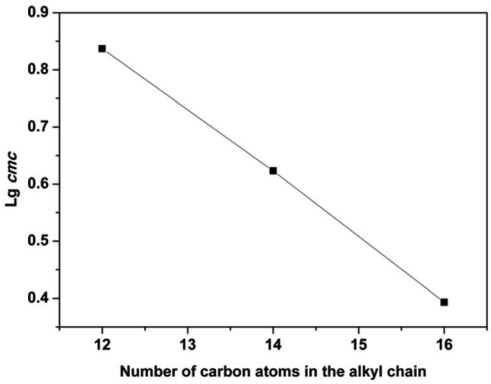


Fig. 2 Influence of the alkyl chain length (*R*) in the cation on the logarithm of cmc.

present in the cations, and ILs 13–15 therefore had an amphiphilic nature. In contrast, others (ILs 1–12) which lack long alkyl chains and did not form micelles, and just behaved as simple salts.[36] For ILs 13–15, the critical micelle concentration (cmc, a breakpoint in the surface tension $\gamma$–log *C* plots) values were found to range from 2.43 to 6.87 mmol $L^{-1}$ (Table 1), closer to that of new 4° ammonium surfactants *N*-alkyl-*N*,*N*-2-dihydroxyethyl-*N*-methylammonium bromides ($C_n$DHAB, $n$ = 12, 14 or 16).[37] Additionally, as the alkyl chain in the hydrophobic portion was linearly elongated from 12 to 16, the cmc was decreased from 6.87 mmol $L^{-1}$ for IL 13 to 12.43 mmol $L^{-1}$ for IL 15. The relationship between log cmc and the alkyl chain length, presented in Fig. 2, followed the Stauff–Klevens rule.[38] The surface tension at cmc ($\gamma_{cmc}$) was also decreased, which is consistent with the cmc decreasing in the same order.

The lower the cmc or $\gamma_{cmc}$ value, the higher surface activity. These values for ILs 13–15 were markedly lower than those of alkyltrimethylammonium chloride (($C_n$TMA)Cl, $n$ = 12, 14 or 16), which are well known as agricultural wetting agents for regulating the properties of herbicidal spray solution, such as the wettability, spreadability and permeability,[39] thus demonstrating that ILs 13–15 were superior to these agents. Nevertheless, two flexible hydroxylethyl groups can easily interact with plant membranes through hydrogen bonding or electrostatic interaction, enabling their permeabilization.

## 2.3 Herbicidal activity

**2.3.1 Preliminary of herbicidal potential study.** Initially, the herbicidal potential of ILs was assessed by standard pre- and postemergence treatments under greenhouse conditions – an important consideration in herbicide development. The selected weed species include one grass *E. indica* and five broadleaf weeds *A. retroflexus*, *E. prostrata*, *X. sibiricum*, *C. album* and *S. nigrum*, which have become major problematic weeds in the cotton fields in Northern China.

The results of the greenhouse studies are summarized in Table S2.† All ILs tested showed no pre emergence herbicidal activities, even at concentrations up to 15 mg $mL^{-1}$, in that the weed seeds germinated and grew normally to the water control. However, when post emergence was applied, differential herbicidal activities were observed for the ILs. Among them, ILs 13–15 showed a complete post emergence herbicidal activity against five broadleaf weeds, and only a slight activity against grass *E. indica*, whereas other salts (ILs 1–12) had either limited or no herbicidal effect, and even had growth promoting effect towards weeds at the highest concentration (*e.g.*, ILs 8, 10 and 11). It illustrated that the herbicidal activity was closely associated with alkyl chains length and the degree of substitution of the ammonium cation. Apparently, the long alkyl chain substituents attached on the 4° ammonium cations, as in ILs 13–15, seemed to significantly affect the herbicidal activity, mainly due to their higher surface effect. Long chain in ILs 13–15 can enhance their wetting, spreading or permeating abilities by lowering the surface tension, which allow more absorption by weed plants, potentially disrupting the plant membranes and causing stronger herbicidal effects. This hypothesis was supported by the facts of those long-chained HILs.[7–18]

In addition, some differences in the herbicidal selectivity by ILs 13–15 between two weed species was also observed, which

Table 1 Surface properties of ILs 13–15 in aqueous solution at 298 K

| IL | cmc (mM) | $\gamma_{cmc}$ (mN $m^{-1}$) | $\Gamma_{max}$[a] (μmol $m^{-2}$) | $A_{min}$[b] ($nm^2$) | $pC_{20}$[c] | $\Pi_{cmc}$ (mN $m^{-1}$) |
|---|---|---|---|---|---|---|
| 13 | 6.46 | 32.46 | 1.30 | 1.279 | 3.04 | 39.84 |
| 14 | 3.92 | 31.11 | 1.33 | 1.243 | 3.37 | 41.19 |
| 15 | 2.35 | 28.66 | 1.34 | 1.238 | 3.84 | 43.64 |

[a] $\Gamma_{max}$ – maximum adsorption. [b] $A_{min}$ – minimum area per surfactant molecule at the air–water interface were calculated by using the Gibbs absorption equation. [c] $pC_{20}$ – efficiency of surface adsorption on an air–water interface.

 

was dependent on both the leaf surface differences[40,41] and the hydrophilic nature for ILs 13–15 with HLB values in the range of 8.14–9.56. Since grass *E. indica* exhibited hydrophobicity with a greater epicuticular wax deposition 0.5 μm thick,[42] the large and isolated drops were formed and rolled off the leave surface after spraying, thereby leading to less of such salts being absorbed. This might be the reason why *E. indica* was more tolerant to ILs 13–15.

**2.3.2 Further herbicidal activity study.** In a preliminary screening of the herbicidal potential of ILs, only ILs 13–15 completely controlled the broadleaf weeds but could not successfully control the grass weed when post emergence was applied, whereas others were not highly active. Therefore, ILs 13–15 were chosen for further post emergence activity against some broadleaf weeds, including *C. album*, *S. nigrum* and *X. sibiricum*, using DCA as a positive control.

It was shown that ILs 13–15 exhibited clear concentration-dependent herbicidal effects, which was enhanced with an increasing IL concentration from 1.25 to 15 mg $mL^{-1}$ (Table 2 and Fig. S32–S43†). After spray application, they caused the weed seedlings to become yellow, stunt, fold, wither, and eventually led to weed death. These symptoms of toxicity became more severe when the concentration was applied above 2.5 mg $mL^{-1}$. To quantify the herbicidal efficacies, the $EC_{50}$ values were calculated after 21 days of spraying. The $EC_{50}$ values of ILs 13–15 were in the range of 1.74–2.95 mg $mL^{-1}$ for *C. album*, 2.46–4.40 mg $mL^{-1}$ for *S. nigrum*, and 1.12–2.66 mg $mL^{-1}$ for *X. sibiricum*. In either case, the $EC_{50}$ values increased linearly with extending alkyl chain lengths (Fig. 3), meaning that elongation of the alkyl chain decreased the herbicidal activity. Since the larger steric hindrance from a longer alkyl chain prevents penetration across cuticular membranes,[43] the herbicidal activity is decreased as a result.

Significantly, the $EC_{50}$ values for ILs 13–15 were 1.7–10.8 folds of magnitude below those of the anionic precursor DCA (Table 2), which proved to be less active due to its photolysis nature. The herbicidal enhancement was indeed achieved by ILs 13–15 by using the HIL strategy. It was concluded that the structural conversion of DCA into an ionic salt form leads to the enhancement of herbicidal activity, which might be a consequence of the synergistic effect of structural factors *per se*, *e.g.*, surface activity, solubility, and stability. Depending on their stable ionic structures, ILs 13–15 possess a requisite stability to undergo less photolysis, thus leading to a high photochemical stability. Moreover, no amide formation was observed after three months of storage in an ambient light at room temperature for ILs 13–15. It was also demonstrated that no reduction in herbicidal activity was observed under the same conditions.

Furthermore, ILs 13–15 took a shorter time than DCA to reach a maximal efficiency, *e.g.*, at 7.5 mg $mL^{-1}$ during the first 7 days after spraying (Fig. 4), again likely due to structural factors that promote the rates of cuticular penetration and/or uptake of these active salts.[35,44] In addition, ILs 13–15 had a quicker response than glyphosate (isopropylamine salt), which belongs to systemic herbicides.[4] For glyphosate treatment with the same time period, there was no clear herbicidal effect on weeds (data were not shown).

### 2.4 Crop selectivity

ILs 13–15 were also tested for phytotoxicity effects on the growth of cotton plants (Zhongmiansuo 79) under greenhouse conditions. The results showed that when ILs 13–15 were applied at the highest concentration of 15 mg $mL^{-1}$, they damaged the growth of cotton and caused relatively severe phytotoxicity effects (stalk browning, leaf burning, necrosis, wilting). At lower concentrations, the slightly injured cotton can recover from the initial injury during the growth. Moreover, the selectivity index (SI) values of ILs 13–15 between cotton plants and three broadleaf weeds were identified. The SI values of ILs 13–15 ranged from 0.443 to 3.67 (Fig. 5). The more SI increases above 1, the more selective the herbicide is between the crop and the weeds, and An SI above 2 means that an herbicide could safely

Table 2 Comparison of the postemergence herbicidal activity of ILs 13–15 *versus* DCA against some broadleaf weeds in the greenhouse

| | | Fresh weight inhibition[a] (%) at 21 days after spraying | | | | | | |
|---|---|---|---|---|---|---|---|---|
| Broadleaf weeds | Compd. | 1.25 (mg $mL^{-1}$) | 2.5 (mg $mL^{-1}$) | 5 (mg $mL^{-1}$) | 7.5 (mg $mL^{-1}$) | 10 (mg $mL^{-1}$) | 15 (mg $mL^{-1}$) | $EC_{50}$[b] (95% CL) (mg $mL^{-1}$) |
| *C. album* | IL 13 | 34.80 ± 2.34a | 65.68 ± 2.30a | 90.23 ± 1.48a | 99.49 ± 0.87a | 100 ± 0a | 100 ± 0a | 1.74 (1.32–2.14) |
| | IL 14 | 27.43 ± 5.28 ab | 47.63 ± 4.52b | 84.41 ± 1.10b | 96.77 ± 2.79a | 99.74 ± 0.44a | 100 ± 0a | 2.22 (1.58–2.87) |
| | IL 15 | 16.76 ± 5.43bc | 39.29 ± 2.31c | 67.56 ± 2.22c | 89.69 ± 3.63b | 98.11 ± 3.26a | 100 ± 0a | 2.95 (3.137–3.50) |
| | DCA | 8.23 ± 2.32c | 19.53 ± 2.95d | 38.44 ± 2.16d | 62.11 ± 2.25c | 86.78 ± 2.72b | 99.74 ± 0.44a | 5.08 (3.32–7.12) |
| *S. nigrum* | IL 13 | 24.73 ± 5.46a | 42.89 ± 3.90a | 74.29 ± 6.85a | 98.75 ± 6.85a | 99.89 ± 0.18a | 100 ± 0a | 2.46 (1.41–3.57) |
| | IL 14 | 10.7 ± 1.71b | 35.7 ± 3.75 ab | 68.49 ± 2.08a | 92.22 ± 4.15a | 99.84 ± 0.27a | 100 ± 0a | 3.13 (2.36–3.94) |
| | IL 15 | 2.21 ± 1.11b | 28.82 ± 1.99b | 40.60 ± 2.56b | 76.9 ± 1.19b | 99.65 ± 0.59a | 100 ± 0a | 4.40 (2.36–6.61) |
| | DCA | 7.58 ± 1.29b | 15.24 ± 2.28c | 27.21 ± 2.18c | 37.00 ± 4.24c | 41.5 ± 4.89b | 72.95 ± 5.52b | 10.00 (7.51–15.71) |
| *X. sibiricum* | IL 13 | 41.10 ± 7.04a | 76.20 ± 1.48a | 96.94 ± 2.65a | 100 ± 0a | 100 ± 0a | 100 ± 0a | 1.12 (0.75–1.59) |
| | IL 14 | 23.7 ± 3.15b | 54.65 ± 5.13b | 97.67 ± 4.02a | 98.8 ± 2.07 ab | 100 ± 0a | 100 ± 0a | 2.16 (4.54–2.74) |
| | IL 15 | 19.5 ± 2.90b | 41.22 ± 3.13c | 76.09 ± 1.41b | 92.9 ± 1.18b | 98.69 ± 2.25a | 100 ± 0a | 2.66 (2.09–3.24) |
| | DCA | −10.5 ± 5.53c | 4.66 ± 3.47d | 13.32 ± 2.81c | 24.89 ± 4.33c | 41.8 ± 3.96b | 58.56 ± 2.38b | 12.46 (11.06–14.61) |

[a] All data represent mean ± SD values, $n = 3$. The small letters were significant differences ($P < 0.05$) according to Tukey's multiple post hoc test by ANOVA. [b] $EC_{50}$ was the 50% inhibition in fresh weight of target weeds.

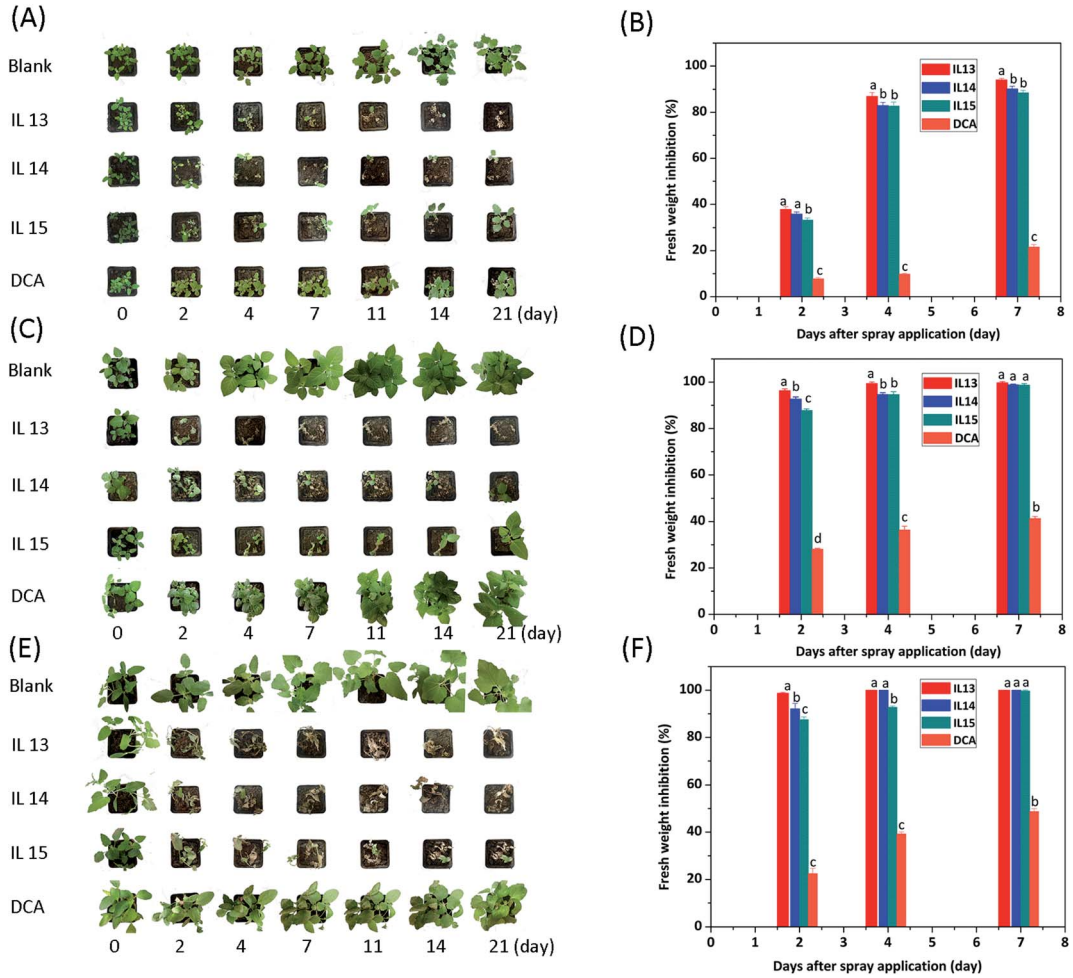


Fig. 3 (A, C and E) The image of the response of *C. album*, *S. nigrum* and *X. sibiricum* after different treatments at 7.5 mg $mL^{-1}$. (B, D and F) Fresh weight inhibition rates of different treatments to *C. album*, *S. nigrum* and *X. sibiricum* after 2, 4, 7 days spraying, respectively. The small letters were significant differences ($P < 0.05$), $n = 3$.

be used in a crop.[45] It was noted that only IL 13 was safe for cotton against these broadleaf weeds when applied post-emergence, with favorable SI values above 2. In addition, the SI values of IL 13 were generally higher than that of IL 14 and IL 15; it indicated that IL 13 was safer than IL 14 and IL 15. Furthermore, IL 13 was also safer than DCA, because the SI values of which were just in the range of 0.16–0.863.

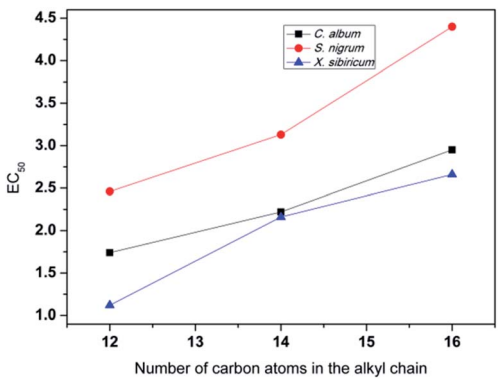


Fig. 4 Influence of the alkyl chain length ($R$) in the cation on $EC_{50}$ values.

## 3 The herbicidal mechanism study

Here, to elucidate the mechanism of action of IL 13 in PS II, Chl a fluorescence induction curve OJIP[46] of *C. album* was studied, using water as a control (Fig. 6). The DCA- and IL 13 treated leaves exhibited different induction curves compared to control. At DCA treatment for 24 h, a slight rise in fluorescence during the first OJ phase was detected, because the electron transport from $Q_A$ to $Q_B$ was partially blocked by DCA resulting in a small amount of $QA^-$ accumulation.[47] Whereas, IL 13 treatment decreased the fluorescence intensity of polyphaser (J–I–P). At IP phase, the intensity of IL 13-treated leaves was much lower than that of water-treated leaves. It suggested that IL 13 caused the PS II center damage leading to decreased excitation energy transfer from the antenna to the reaction center.[48] The damage to PS II center can be detected from the decreases in maximal PS II quantum yield $F_v/F_m$ and the performance index $PI_{abs}$. The values of $F_v/F_m$ and $PI_{abs}$ of IL 13-treated leaves were decreased

 

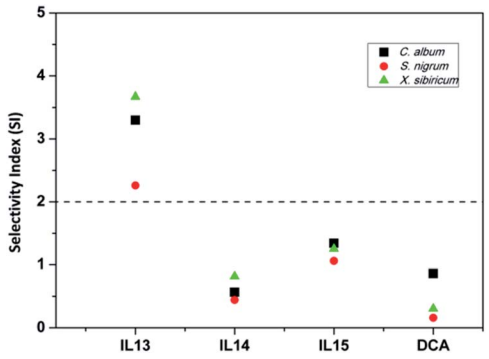


Fig. 5 Selectivity index expressed as the ratio of the $EC_{10}$ value for cotton and the $EC_{90}$ value for weeds.

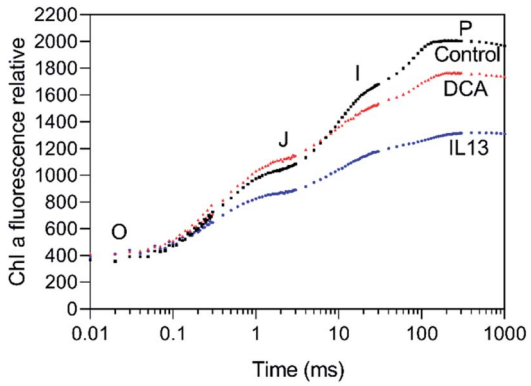


Fig. 6 Effects of IL 13 and DCA on the chlorophyll fluorescence induction curves of a dark-adapted *C. album* leaf.

by 18% and 70%, respectively. In the radar plot (Fig. 7), IL 13 caused the decreases in $TR_0$/RC, $ET_0$/RC, $RE_0$/RC, associated to the decrease of $\varphi p_o$, $\psi E_o$ and $\varphi E_o$, which resulted in the decrease of $PI_{abs}$. A further confirmation of PS II center damage is the reduction in the area size above the fluorescence curve between $F_o$ and $F_m$. The area size was decreased by 38.7% compared to control, indicating that the electron transfer to quinone pool

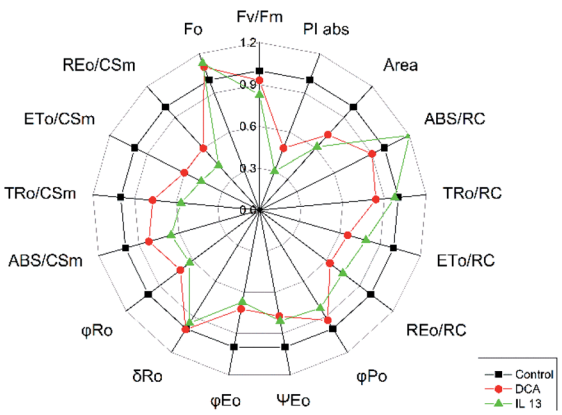


Fig. 7 Radar plot graphs showing the effects of IL 13 on some chlorophyll a fluorescence parameter calculated from OJIP curve.

size of was blocked.[49] Additionally, the damage of PS II structure and function also led to a characteristic rise of $F_o$,[50,51] the value of which was increased by 12.9% relative to control. These results suggested that IL 13 was possibly a novel PS II inhibitor by interrupting electron transport between $Q_A$ and $Q_B$, which can cause the death of weed plants. Furthermore, most fluorescence parameters of IL 13 were lower than the DCA treatment, which consisted with the enhanced herbicidal activity of IL 13 when compared to DCA.

# 4 Conclusions

HIL strategy can be used for designing novel ammonium dichloroacetates ILs, which combine dichlorocetate anion with ammonium cations. The results demonstrated that ionic structure strong influenced the solubility and stability of ILs. Notably, three salts ILs 13–15 with longer alkyl chains preserved the surface activity of the cations, thus enhanced post-emergence herbicidal activity against some broadleaf weeds and accelerated weed death than DCA. Moreover, the further crop safety experiment indicated IL 13 had better safety for cotton in controlling some broadleaf weeds. Chlorophyll a fluorescence measurements indicated that the action mechanism of IL 13 seemed to inhibit electron transport between $Q_A$ and $Q_B$ of PS II. To our knowledge, this is the first example of ammonium dichloroacetates, which shows herbicidal activity against broadleaf weeds in agriculture.

# 5 Experimental section

## 5.1 Materials and methods

Methanol, acetonitrile, acetone, isopropanol, and dimethyl sulfoxide (DMSO), toluene, diethyl ether, and potassium hydroxide were of analytical grade and purchased from Energy Chemical Co., Ltd. (Shanghai, China). The above agents were used without further distillation. Dichloroacetic acid (CAS no. 79-43-6), 1-bromododecane (CAS no. 143-15-7), 1-bromotetradecane (CAS no. 112-71-0), 1-bromohexadecane (CAS no. 112-82-3) and hydroxylalkylamines were purchased from Energy Chemicals (Shanghai, China). Glyphosate isopropylamine salt (purity 62%, aqueous solution) was obtained from Lier Chemical Co., Ltd (Sichuan, China). *N*-Alkyl-*N*,*N*-2-dihydroxyethyl-*N*-methylammonium bromide ($C_n$DHAB, $n$ = 12, 14 and 16) were synthesized according to reported procedures described in the literature.[45] Methyl sulfoxide-$d_6$ with a deuteration degree of 99.8% for NMR spectra was obtained from J & K Scientific Co., Ltd. (Beijing, China).

The $^1$H, $^{13}$C NMR spectra were recorded with a Bruker 400 spectrometer (Bruker, Germany) at 400 and 100 MHz, respectively. Chemical shifts ($\delta$) are reported relative to the residual solvent resonances of methyl sulfoxide-$d_6$.

## 5.2 Synthesis of ammonium dichloroacetates ILs 1–15

Fifteen ammonium dichloroacetates ILs were synthesized through acid–base neutralization but in two different synthetic routes.

**5.2.1 Route I (preparation of ILs 1–12).** Hydroxylalkylamines (0.01 mol) dissolved in methanol (20 mL) was added to a round-bottom flask equipped with a magnetic stirrer. Next, 0.011 mol of dichloroacetic acid was added dropwise and the mixture was stirred at room temperature for 24 h. Methanol was removed *via* rotary evaporation, and the desirable product was thoroughly washed with diethyl ether and finally dried under a reduced pressure at 50 °C for 24 h.

**5.2.2 Route II (preparation of ILs 13–15).** A total of 0.01 mol of quaternary ammonium bromide was first dissolved in methanol and a stoichiometric amount of saturated methanol solution of potassium hydroxide was added. The anion exchange progress was monitored with the addition of an $AgNO_3$ solution. Upon completing the substitution of bromide *via* hydroxide, no AgBr precipitation could be found. The by-product (KBr) was precipitated and separated *via* filtration through a sintered glass filter (Synthware Co., Ltd, Beijing, China). Then, the filter (quaternary ammonium hydroxide) was transferred to a round-bottom flask equipped with a magnetic stirrer and was neutralized with dichloroacetic acid at a 1 : 1.1 molar ratio. The mixture was stirred at room temperature for another 24 h. Methanol was removed *via* rotary evaporation, followed by adding diethyl ether to the residue. After removing the solvents by evaporation, the desirable product was obtained and finally dried under a reduced pressure at 50 °C for 24 h.

### 5.3 Physicochemical data

**5.3.1 IL 1.** Yield: 98%; light yellow solid; mp: 68.0–68.8 °C; $^1$H NMR (400 MHz, DMSO-d$_6$) $\delta$ (ppm) = 2.84 (t, 2H, $^3J_{H-H}$ = 8.0 Hz, C$\underline{H}_2$), 3.57 (t, 2H, $^3J_{H-H}$ = 8.0 Hz, C$\underline{H}_2$), 5.30 (s, br, 1H, O$\underline{H}$), 5.91 (s, 1H, C$\underline{H}$Cl), 7.98 (s, br, 3H, N$\underline{H}_3^+$); $^{13}$C NMR (100 MHz, DMSO-d$_6$) $\delta$ (ppm) = 41.28 (C$\underline{H}_2$), 57.65 (C$\underline{H}_2$), 70.84 (C$\underline{H}$Cl$_2$), 165.50 (C$\underline{O}$O$^-$).

**5.3.2 IL 2.** Yield: 95%; white solid; mp: 109.8–110.8 °C; $^1$H NMR (400 MHz, DMSO-d$_6$) $\delta$ (ppm) = 1.08 (d, 3H, $^3J_{H-H}$ = 4.0 Hz, C$\underline{H}_3$), 2.60 (m, 1H, C$\underline{H}_2$), 2.82 (dd, 1H, $^3J_{H-H}$ = 8.0 Hz, 4.0 Hz, C$\underline{H}_2$), 3.82 (m, 1H, C$\underline{H}$), 5.44 (s, br, 1H, O$\underline{H}$), 5.94 (s, 1H, C$\underline{H}$Cl), 8.08 (s, br, 3H, N$\underline{H}_3^+$); $^{13}$C NMR (100 MHz, DMSO-d$_6$) $\delta$ (ppm) = 20.97 (C$\underline{H}_3$), 45.66 (C$\underline{H}_2$), 63.14 (C$\underline{H}$), 70.83 (C$\underline{H}$Cl$_2$), 165.50 (C$\underline{O}$O$^-$).

**5.3.3 IL 3.** Yield: 97%; light yellow liquid; $^1$H NMR (400 MHz, DMSO-d$_6$) $\delta$ (ppm) = 1.69 (quint, 2H, $^3J_{H-H}$ = 8.0 Hz, C$\underline{H}_2$), 2.84 (t, 2H, $^3J_{H-H}$ = 8.0 Hz, C$\underline{H}_2$), 3.47 (t, 2H, $^3J_{H-H}$ = 8.0 Hz, C$\underline{H}_2$), 4.84 (s, br, 1H, O$\underline{H}$), 5.90 (s, 1H, C$\underline{H}$Cl), 7.95 (s, br, 3H, N$\underline{H}_3^+$); $^{13}$C NMR (100 MHz, DMSO-d$_6$) $\delta$ (ppm) = 30.17 (C$\underline{H}_2$), 36.64 (C$\underline{H}_2$), 57.93 (C$\underline{H}_2$), 71.00 (C$\underline{H}$Cl$_2$), 165.09 (C$\underline{O}$O$^-$).

**5.3.4 IL 4.** Yield: 97%; light yellow liquid; $^1$H NMR (400 MHz, DMSO-d$_6$) $\delta$ (ppm) = 2.96 (t, 2H, $^3J_{H-H}$ = 4.0 Hz, C$\underline{H}_2$), 3.45 (t, 2H, $^3J_{H-H}$ = 4.0 Hz, C$\underline{H}_2$), 3.51 (t, 2H, $^3J_{H-H}$ = 8.0 Hz, C$\underline{H}_2$), 3.59 (t, 2H, $^3J_{H-H}$ = 8.0 Hz, C$\underline{H}_2$), 5.92 (s, 1H, C$\underline{H}$Cl), 7.19 (s, br, 3H, N$\underline{H}_3^+$); $^{13}$C NMR (100 MHz, DMSO-d$_6$) $\delta$ (ppm) = 38.74 (C$\underline{H}_2$), 60.17 (C$\underline{H}_2$), 66.67 (C$\underline{H}_2$), 70.81 (C$\underline{H}_2$), 72.26 (C$\underline{H}$Cl$_2$), 165.57 (C$\underline{O}$O$^-$).

**5.3.5 IL 5.** Yield: 96%; light yellow liquid; $^1$H NMR (400 MHz, DMSO-d$_6$) $\delta$ (ppm) = 2.54 (s, 3H, C$\underline{H}_3$), 2.95 (t, 2H, $^3J_{H-H}$ = 8.0 Hz, C$\underline{H}_2$), 3.63 (t, 2H, $^3J_{H-H}$ = 8.0 Hz, C$\underline{H}_2$), 5.48 (s, br, 1H, O$\underline{H}$), 5.97 (s, 1H, C$\underline{H}$Cl), 8.99 (s, br, 2H, N$\underline{H}_2^+$); $^{13}$C NMR (100 MHz, DMSO-d$_6$) $\delta$ (ppm) = 32.71 (C$\underline{H}_3$), 50.56 (C$\underline{H}_2$), 56.47 (C$\underline{H}_2$), 70.47 (C$\underline{H}$Cl$_2$), 166.45 (C$\underline{O}$O$^-$).

**5.3.6 IL 6.** Yield: 98%; light yellow liquid; $^1$H NMR (400 MHz, DMSO-d$_6$) $\delta$ (ppm) = 0.87 (t, 3H, $^3J_{H-H}$ = 8.0 Hz, C$\underline{H}_3$), 1.31 (sext, 2H, C$\underline{H}_2$), 1.57 (m, 2H, C$\underline{H}_2$), 2.85 (m, 2H, C$\underline{H}_2$), 2.94 (t, 2H, $^3J_{H-H}$ = 4.0 Hz, C$\underline{H}_2$), 3.63 (t, 2H, $^3J_{H-H}$ = 8.0 Hz, C$\underline{H}_2$), 5.40 (s, br, 1H, OH), 5.93 (s, 1H, C$\underline{H}$Cl), 8.45 (s, br, 2H, N$\underline{H}_2^+$); $^{13}$C NMR (100 MHz, DMSO-d$_6$) $\delta$ (ppm) = 13.55 (C$\underline{H}_3$), 19.35 (C$\underline{H}_2$), 27.40 (C$\underline{H}_2$), 46.59 (C$\underline{H}_2$), 48.90 (C$\underline{H}_2$), 56.47 (C$\underline{H}_2$), 70.51 (C$\underline{H}$Cl$_2$), 165.43 (C$\underline{O}$O$^-$).

**5.3.7 IL 7.** Yield: 93%; light yellow liquid; $^1$H NMR (400 MHz, DMSO-d$_6$) $\delta$ (ppm) = 1.08 (dd, 6H, $^3J_{H-H}$ = 8.0 Hz, 4.0 Hz, C$\underline{H}_3$), 2.76 (m, 4H, C$\underline{H}_2$), 2.96 (m, 2H, C$\underline{H}_2$), 3.95 (m, 2H, C$\underline{H}$), 5.25 (s, br, 2H, O$\underline{H}$), 5.97 (s, 1H, C$\underline{H}$Cl), 8.63 (s, br, 2H, N$\underline{H}_2^+$); $^{13}$C NMR (100 MHz, DMSO-d$_6$) $\delta$ (ppm) = 21.18 (C$\underline{H}_3$), 53.68 (C$\underline{H}_2$), 62.03 (C$\underline{H}$), 70.52 (C$\underline{H}$Cl$_2$), 165.46 (C$\underline{O}$O$^-$).

**5.3.8 IL 8.** Yield: 99%; light yellow liquid; $^1$H NMR (400 MHz, DMSO-d$_6$) $\delta$ (ppm) = 2.80 (s, 3H, C$\underline{H}_3$), 3.19 (t, 4H, $^3J_{H-H}$ = 8.0 Hz, C$\underline{H}_2$), 3.73 (t, 4H, $^3J_{H-H}$ = 8.0 Hz, C$\underline{H}_2$), 4.23 (s, br, 2H, O$\underline{H}$), 6.02 (s, 1H, C$\underline{H}$Cl), 9.98 (s, br, 1H, N$\underline{H}^+$); $^{13}$C NMR (100 MHz, DMSO-d$_6$) $\delta$ (ppm) = 40.56 (C$\underline{H}_3$), 55.43 (C$\underline{H}_2$), 57.49 (C$\underline{H}_2$), 70.13 (C$\underline{H}$Cl$_2$), 166.03 (C$\underline{O}$O$^-$).

**5.3.9 IL 9.** Yield: 94%; light yellow liquid; $^1$H NMR (400 MHz, DMSO-d$_6$) $\delta$ (ppm) = 1.16 (t, 6H, $^3J_{H-H}$ = 8.0 Hz, C$\underline{H}_3$), 3.06 (t, 6H, $^3J_{H-H}$ = 8.0 Hz, C$\underline{H}_2$), 3.70 (t, 6H, $^3J_{H-H}$ = 8.0 Hz, C$\underline{H}_2$), 5.65 (s, br, 2H, O$\underline{H}$, N$\underline{H}^+$), 5.98 (s, 1H, C$\underline{H}$Cl$_2$); $^{13}$C NMR (100 MHz, DMSO-d$_6$) $\delta$ (ppm) = 8.84 (C$\underline{H}_3$), 46.92 (C$\underline{H}_2$), 53.18 (C$\underline{H}_2$), 55.93 (C$\underline{H}_2$), 70.44 (C$\underline{H}$Cl$_2$), 166.32 (C$\underline{O}$O$^-$).

**5.3.10 IL 10.** Yield: 92%; white solid; mp: 67.4 °C; $^1$H NMR (400 MHz, DMSO-d$_6$) $\delta$ (ppm) = 3.09 (t, 6H, $^3J_{H-H}$ = 4.0 Hz, C$\underline{H}_2$), 3.66 (t, 6H, $^3J_{H-H}$ = 4.0 Hz, C$\underline{H}_2$), 5.26 (s, br, 3H, O$\underline{H}$), 5.95 (s, 1H, C$\underline{H}$Cl); $^{13}$C NMR (100 MHz, DMSO-d$_6$) $\delta$ (ppm) = 55.81 (C$\underline{H}_2$), 56.43 (C$\underline{H}_2$), 70.70 (C$\underline{H}$Cl$_2$), 165.63 (C$\underline{O}$O$^-$).

**5.3.11 IL 11.** Yield: 90%; light yellow solid; mp: 63.8–68.0 °C; $^1$H NMR (400 MHz, DMSO-d$_6$) $\delta$ (ppm) = 1.08 (d, 9H, $^3J_{H-H}$ = 8.0 Hz, C$\underline{H}_3$), 3.12 (m, 6H, C$\underline{H}_2$), 4.06 (m, 3H, C$\underline{H}$), 4.68 (s, br, 3H, O$\underline{H}$), 6.05 (s, 1H, CHCl); $^{13}$C NMR (100 MHz, DMSO-d$_6$) $\delta$ (ppm) = 20.91 (C$\underline{H}_3$), 21.41 (C$\underline{H}_3$), 21.60 (C$\underline{H}_3$), 60.14 (C$\underline{H}$), 60.81 (C$\underline{H}$), 61.15(C$\underline{H}_2$), 61.83 (C$\underline{H}_2$), 69.99 (C$\underline{H}$Cl$_2$), 165.59 (C$\underline{O}$O$^-$).

**5.3.12 IL 12.** Yield: 90%; yellow liquid; $^1$H NMR (400 MHz, DMSO-d$_6$) $\delta$ (ppm) = 3.12 (s, 9H, C$\underline{H}_3$), 3.06 (t, 2H, $^3J_{H-H}$ = 4.0 Hz, C$\underline{H}_2$), 3.82 (m, 2H, C$\underline{H}_2$), 5.92 (s, br, 1H, O$\underline{H}$), 5.85 (s, 1H, C$\underline{H}$Cl); $^{13}$C NMR (100 MHz, DMSO-d$_6$) $\delta$ (ppm) = 38.89 (C$\underline{H}_3$), 55.43 (C$\underline{H}_2$), 57.49 (C$\underline{H}_2$), 70.13 (C$\underline{H}$Cl$_2$), 166.03 (C$\underline{O}$O$^-$).

**5.3.13 IL 13.** Yield: 94%; white solid; mp: 38.9 °C; $^1$H NMR (400 MHz, DMSO-d$_6$) $\delta$ (ppm) = 0.84 (t, 3H, $^3J_{H-H}$ = 8.0 Hz, C$\underline{H}_3$), 1.23 (m, 16H, C$\underline{H}_2$), 1.66 (m, 2H, C$\underline{H}_2$), 3.08 (s, 3H, C$\underline{H}_3$), 3.39 (m, 4H, C$\underline{H}_2$), 3.43 (m, 4H, C$\underline{H}_2$), 3.81 (m, 4H, C$\underline{H}_2$), 5.67 (s, br, 2H, OH), 5.83 (s, 1H, C$\underline{H}$Cl); $^{13}$C NMR (100 MHz, DMSO-d$_6$) $\delta$ (ppm) = 14.05 (C$\underline{H}_3$), 21.66 (C$\underline{H}_2$), 22.19 (C$\underline{H}_2$), 25.88 (C$\underline{H}_2$), 28.60 (C$\underline{H}_2$), 28.80 (C$\underline{H}_2$), 28.92 (C$\underline{H}_2$), 29.02 (C$\underline{H}_2$), 29.10 (C$\underline{H}_2$), 31.38 (C$\underline{H}_2$), 49.05 (C$\underline{H}_3$), 54.83 (C$\underline{H}_2$), 58.87 (C$\underline{H}_2$), 59.92 (C$\underline{H}_2$), 62.45 (C$\underline{H}_2$), 63.25 (C$\underline{H}_2$), 71.41 (C$\underline{H}$Cl$_2$), 164.43 (C$\underline{O}$O$^-$).

**5.3.14 IL 14.** Yield: 93%; white solid; mp: 52.3–53.6 °C; $^1$H NMR (400 MHz, DMSO-d$_6$) $\delta$ (ppm) = 0.85 (t, 3H, $^3J_{H-H}$ = 8.0 Hz,

$C\underline{H}_3$), 1.23 (m, 20H, $C\underline{H}_2$), 1.66 (m, 2H, $C\underline{H}_2$), 3.07 (s, 3H, $C\underline{H}_3$), 3.40 (s, 8H, $C\underline{H}_2$), 3.81 (m, 4H, $C\underline{H}_2$), 5.43 (s, br, 2H, OH), 5.80 (s, 1H, $C\underline{H}Cl$); $^{13}$C NMR (100 MHz, DMSO-$d_6$) $\delta$ (ppm) = 14.04 ($\underline{C}H_3$), 21.64 ($\underline{C}H_2$), 22.17 ($\underline{C}H_2$), 25.86 ($\underline{C}H_2$), 28.58 ($\underline{C}H_2$), 28.78 ($\underline{C}H_2$), 28.89 ($\underline{C}H_2$), 29.01 ($\underline{C}H_2$), 29.08 ($\underline{C}H_2$), 29.13 ($\underline{C}H_2$), 31.36 ($\underline{C}H_2$), 49.02 ($\underline{C}H_3$), 54.82 ($\underline{C}H_2$), 58.54 ($\underline{C}H_2$), 59.65 ($\underline{C}H_2$), 62.43 ($\underline{C}H_2$), 63.22 ($\underline{C}H_2$), 71.57 ($\underline{C}HCl_2$), 164.04 ($\underline{C}OO^-$).

**5.3.15 IL 15.** Yield: 90%; white solid; mp: 80.9–81.8 °C; $^1$H NMR (400 MHz, DMSO-$d_6$) $\delta$ (ppm) = 0.85 (t, 3H, $^3J_{H-H}$ = 8.0 Hz, $C\underline{H}_3$), 1.23 (m, 26H, $C\underline{H}_2$), 1.66 (m, 2H, $C\underline{H}_2$), 3.07 (s, 3H, $C\underline{H}_3$), 3.37 (s, 4H, $C\underline{H}_2$), 3.43 (m, 4H, $C\underline{H}_2$), 3.80 (m, 4H, $C\underline{H}_2$), 5.40 (s, br, 2H, OH), 5.82 (s, 1H, $C\underline{H}Cl$); $^{13}$C NMR (100 MHz, DMSO-$d_6$) $\delta$ (ppm) = 20.82 ($\underline{C}H_3$), 21.38 ($\underline{C}H_2$), 21.56 ($\underline{C}H_2$), 60.33 ($\underline{C}H_3$), 61.06 ($\underline{C}H_2$), 61.40 ($\underline{C}H_2$), 62.00 ($\underline{C}H_2$), 70.47 ($\underline{C}HCl_2$), 165.28 ($\underline{C}OO^-$).

### 5.4 Solubilities

The solubilities of the ILs in eight representative solvents were determined according to the protocols in Vogel's Textbook of Practical Organic Chemistry.[52] The solvents were selected for analyses and arranged in decreasing order of Snyder polarity index: water, 9.0; methanol, 6.6; DMSO, 6.5; acetonitrile, 6.2; acetone, 5.1; isopropanol, 4.3; diethyl ether, 2.8; and toluene, 2.3. A 0.1 g sample of each salt was added to a certain volume of the solvent. Based on the volume of the solvent used, three types of behaviors were recorded: 'soluble' applies to compounds that dissolved in 1 mL of solvent, 'limited solubility' applies to compounds that dissolved in 3 mL of solvent, and 'not soluble' applies to compounds that did not dissolve in 3 mL of solvent. The treatments were performed at 25 °C.

### 5.5 Surface tension measurement

The surface tension measurements were measured with the platinum ring method using a ZF-2 tensiometer at 298 ± 0.2 K. The tensiometer was calibrated against ultrapure water, which was generally 72.00 ± 0.50 mN m$^{-1}$. The IL solutions in different concentrations were freshly prepared using ultrapure water. The platinum ring was thoroughly cleaned and dried before each measurement. Then the platinum ring was dipped to the solutions at a slow speed and stopped when the surface tension values remained unchanged, indicating that equilibrium had been reached. In all cases, five successive measurements were performed, and the standard deviation did not exceed 0.20 mN m$^{-1}$.

### 5.6 Herbicidal activity assays of ILs 1–15

**5.6.1 Weed species and preparation of the IL solutions.** Herbicidal activity was evaluated against both grass and broadleaf weeds grown in greenhouses: *Eleusine indica* (L.) *Gaertn.*, *Amaranthus retroflexus* L., *Eclipta prostrata*, *Xanthium sibiricum Patr*, *Chenopodium album* L. and *Solanum nigrum* L. The weed seeds were collected from the experimental farm of the Institute of Cotton Research of the Chinese Academy of Agricultural Sciences (CAAS), PR China. These species are malignant weeds that have become problematic in the cotton fields in Northern China.

Each salt was first dissolved in ethanol, and then diluted with deionized water containing 0.1% Tween 80 to form an emulsifiable solution in different concentrations from 1.25 to 15 mg mL$^{-1}$. In greenhouse tests, the solutions were sprayed using a laboratory spray bottle. There were three replicates for each treatment. A mixture of the same amount of deionized water, ethanol plus Tween 80 was used as a blank control. Dichloroacetic acid was applied as a positive control.

**5.6.2 Pre emergence tests.** Loamy sand in plastic pots (5 cm depth) was wetted with water, and ten sprouting seeds of the weeds were planted in earth (0.6 cm depth) in a greenhouse at a temperature of 25 °C, a relative humidity of 60%, and a photoperiod (day/night hours) of 16/8. 2 mL of emulsifiable solution of each salt was applied directly to the surface of the soil using a laboratory spray bottle. Then the pots were placed in a greenhouse, being watered daily.

**5.6.3 Post emergence tests.** After emergence, for the grass species 10 plants were grown *per* pot, but for the larger broadleaf weed species, 3–5 plants were grown in each pot. The seedlings of the weeds at the 4–6 leaf stage were sprayed with the tested salts at different concentrations from 1.25 to 15 mg mL$^{-1}$. Subsequently, the weeds were returned to the greenhouse, being watered daily. Their responses to the individual treatments were recorded at 2, 4, 7, 11, 14, and 21 days after application.

Dichloroacetic acid was applied as a positive control. A similar set of experiments was conducted.

**5.6.4 Data collection.** After 21 days of treatment, the aerial parts of the weeds were harvested and the fresh weights were recorded. The herbicidal efficacies were measured from the fresh weights.

The fresh weight inhibition rates relative to the water blank control was then calculated using the following formula (eqn (1)):

$$\text{Fresh weight inhibition rate (\%)} = (1 - T/C) \times 100 \quad (1)$$

where $T$ is the average fresh weight in the treatment, and $C$ is the average fresh weight in the blank control.

### 5.7 Crop selectivity

The cotton seeds (*Gossypium hirsutum* L.) were planted in plastic pots (5 cm depth) and grown in a greenhouse at a temperature of 25 °C, a relative humidity of 60%, and a photoperiod (day/night hours) of 16/8. When the cottons reached the 4–6 true leaf stage, crop safety experiments were conducted at the same concentrations ranging from 1.25 to 15 mg mL$^{-1}$. After 21 days of treatment, the fresh weight inhibition rates of the cottons were then calculated by using the above formula.

### 5.8 Statistical analysis

Data analyses were conducted using the statistical analysis software (SPSS, Standard Version 16.0, SPSS Inc., USA). The concentration at which 50% inhibition $EC_{50}$ or 90% inhibition $EC_{90}$ and its 95% confidence intervals (weeds), as well as 10% inhibition $EC_{10}$ (cotton) were calculated by probit analyses

based on the logarithm of the concentration *versus* the percent inhibition. All quantitative data were presented as the mean ± SD of at least three independent experiments using the Tukey's multiple post *hoc* test. $P < 0.05$ was considered as a statistically significant difference.

$$EC_{90}(\text{weeds})$$

where $EC_{90}$ equals a 90% effect on the weeds and $EC_{10}$ equals a 10% effect on the crop, respectively.

The more SI increases above 2, the more selective IL becomes in the crop species.

### 5.9 Chlorophyll fluorescence determination

Chlorophyll fluorescence determination was assessed 24 h after spray application of IL 13. Prior to the measurements, *C. album* was kept in the dark for 15 min, then the leaves were excited by saturating red light pulse (3000 μmol $m^{-2}$ $s^{-1}$) from three light-emitting diodes (650 nm). The pulse duration was 1 s. Chlorophyll a fluorescence induction curves (OJIP curves) were measured with a Handy-PEA chlorophyll fluorometer (Plant Efficiency Analyzer, Hansatech, King's Lynn, UK). The JIP-test was used to analyze each chlorophyll a fluorescence parameter. It provided information about biophysical properties of the photosynthetic energy conversion and transport of electrons.[46–51] Some fluorescence parameters were highlighted: (a) area: total complementary area between $F_o$ and $F_m$ (reflecting the size of the plastoquinone pool); where $F_o$ is minimal fluorescence when PSII RCs are all open, $F_m$: maximal fluorescence when PSII RCs are all closed; (b) the specific energy fluxes per reaction center RC for absorbance (ABS/RC), for transport ($ET_0$/RC), for trapping $TR_0$/RC and for reduction ($RE_0$/RC); (c) the phenomenological energy fluxes per excited cross section for absorbance ($ABS/CS_m$), for transport ($ET_o/CS_m$), for trapping ($TR_o/CS_m$) and for reduction ($RE_0/CS_m$); (d) the performance index: $PI_{ABS} = (RC/ABS) \times (\varphi p_o/(1 - \varphi p_o)) \times (\psi E_o/(1 - \psi E_o))$, where, RC is for reaction center; ABS is for absorption flux; $\varphi p_o$ is the maximum yield of primary photochemistry ($\varphi p_o = TR_0/ABS$) and $\psi E_o$ is the probability that a trapped exciton moves an electron into the electron transport chain beyond QA ($\psi E_o = ET_0/TR_0$).

## Conflicts of interest

There are no conflicts to declare.

## Acknowledgements

This study was supported by the Cotton Industrial Technology System of China (grant number CARS-15-20), the National Key Research and Development Plan of China (grant number 2016YFD0200700), and the National Natural Science Foundation of China (grant number 31801751).

## Notes and references

1 (*a*) J. E. Duffus, *Annu. Rev. Phytopathol.*, 1971, **9**, 319; (*b*) F. Dong, J. H. Xu, X. Zhang, S. F. Wang, Y. J. Xing, M. P. Mokoena, A. O. Olaniran and J. R. Shi, *Plant Pathol.*, 2020, 1; (*c*) S. Vennila, Y. G. Prasad, M. Prabhakar, M. Agarwal, G. Sreedevi and O. M. Bambawale, *J. Environ. Biol.*, 2013, **34**, 153; (*d*) X. Peng, L. Liu, X. Guo, P. L. Wang, C. M. Song, S. Su, G. J. Fang and M. H. Chen, *J. Econ. Entomol.*, 2020, **113**, 185.

2 H. Kraehmer, B. Laber, C. Rosinger and A. Schulz, *Plant Physiol.*, 2014, **166**, 1119.

3 B. C. Vieira, J. D. Luck, K. L. Amundsen, R. Werle, T. A. Gaines and G. R. Kruger, *Sci. Rep.*, 2020, **10**, 2146.

4 R. L. Tominack, *Clin. Toxicol.*, 2000, **38**, 129.

5 F. Orellana-García, M. A. Álvarez, V. López-Ramón, J. Rivera-Utrilla, M. Sánchez-Polo and A. J. Mota, *Chem. Eng. J.*, 2014, **255**, 307.

6 C. Délye, M. Jasieniuk and V. L. Corre, *Trends Genet.*, 2013, **29**, 649.

7 J. Pernak, A. Syguda, D. Janiszewska, K. Materna and T. Praczyk, *Tetrahedron*, 2011, **67**, 4838.

8 O. A. Cojocaru, J. L. Shamshina, G. Gurau, A. Syguda, T. Praczyk, J. Pernak and R. D. Rogers, *Green Chem.*, 2013, **15**, 2110.

9 J. Pernak, M. Niemczak, R. Giszter, J. L. Shamshina, G. Gurau, O. A. Cojocaru, T. Praczyk, K. Marcinkowska and R. D. Rogers, *ACS Sustainable Chem. Eng.*, 2014, **2**, 2845.

10 (*a*) I. K. Konstantinou, D. G. Hela and T. A. Albanis, *Environ. Pollut.*, 2006, **141**, 55; (*b*) M. Niemczak, Ł. Chrzanowski, T. Praczyk and J. Pernaka, *New J. Chem.*, 2017, **41**, 8066.

11 J. L. Zhu, G. L. Ding, Y. Liu, B. T. Wang, W. B. Zhang, M. C. Guo, Q. Q. Geng and Y. S. Cao, *Chem. Eng. J.*, 2015, **279**, 472.

12 B. T. Wang, G. L. Ding, J. L. Zhu, W. B. Zhang, M. C. Guo, Q. Q. Geng, D. Guo and Y. S. Cao, *Tetrahedron*, 2015, **71**, 7860.

13 G. Tang, B. T. Wang, G. L. Ding, W. B. Zhang, Y. Liang, C. Fan, H. Q. Dong, J. L. Yang, D. D. Kong and Y. S. Cao, *Sci. Total Environ.*, 2018, **616–617**, 128.

14 P. Bałczewski, R. Biczak, M. Turek, B. Pawłowska, E. Różycka-Sokołowska, B. Marciniak, M. Deska and J. Skalik, *Ecotoxicol. Environ. Saf.*, 2018, **163**, 408.

15 M. Niemczak, R. Giszter, K. Czerniak, K. Marcinkowska and F. Walkiewicz, *RSC Adv.*, 2015, **5**, 15487.

16 J. Pernak, M. Niemczak, J. L. Shamshina, G. Gurau, G. Głowacki, T. Praczyk, K. Marcinkowska and R. D. Rogers, *J. Agric. Food Chem.*, 2015, **63**, 3357.

17 K. Marcinkowska, T. Praczyk, M. Gawlak, M. Niemczak and J. Pernak, *Crop Prot.*, 2017, **98**, 85.

18 A. Syguda, A. Gielnik, A. Borkowski, M. Woźniak-Karczewska, A. Parus, A. Piechalak, A. Olejnik, R. Marecik, Ł. Ławniczak and Ł. Chrzanowski, *New J. Chem.*, 2018, **42**, 9819.

19 A. Syguda, K. Marcinkowska and K. Materna, *RSC Adv.*, 2016, **6**, 63136.

20 H. Choudhary, J. Pernak, J. L. Shamshina, M. Niemczak, R. Giszter, Ł. Chrzanowski, T. Praczyk, K. Marcinkowska, O. A. Cojocaru and R. D. Rogers, *ACS Sustainable Chem. Eng.*, 2017, **5**, 6261.

 

21 J. F. Niu, Z. P. Zhang, J. Y. Tang, G. Tang, J. L. Yang, W. C. Wang, H. Huo, N. Jiang, J. Q. Li and Y. S. Cao, *J. Agric. Food Chem.*, 2018, **66**, 10362.
22 W. C. Wang, Y. Liang, J. L. Yang, G. Tang, Z. Y. Zhou, R. Tang, H. Q. Dong, J. Q. Li and Y. S. Cao, *ACS Sustainable Chem. Eng.*, 2019, **7**, 16620–16628.
23 C. Wang, Y. Liang, J. L. Yang, G. Tang, Z. Y. Zhou, R. Tang, H. Q. Dong, J. Q. Li and Y. S. Cao, *ACS Sustainable Chem. Eng.*, 2019, **7**, 16620.
24 W. C. Wang, J. L. Zhu, G. Tang, H. Huo, W. B. Zhang, Y. Liang, H. Q. Dong, J. L. Yang and Y. S. Cao, *New J. Chem.*, 2019, **43**, 827.
25 Ł. Ławniczak, A. Syguda, A. Borkowski, P. Cyplik, K. Marcinkowska, Ł. Wolko, T. Praczyk, Ł. Chrzanowski and J. Pernak, *Sci. Total Environ.*, 2016, **563–564**, 247.
26 C. A. Schoonjans, N. Joudiou, D. Brusa, C. Corbet, O. Feron and B. Gallez, *Cancer Lett.*, 2020, **470**, 18.
27 D. Stakišaitis, M. Juknevičienė, E. Damanskienė, A. Valanėiūtė, I. Balnytė and M. M. Alonso, *Cancers*, 2019, **11**, 1210.
28 P. W. Stacpoole, E. M. Harman, S. H. Curry, T. G. Baumgartner and R. I. Misbin, *N. Engl. J. Med.*, 1983, **309**, 390.
29 T. Deuse, X. Q. Hua, D. Wang, L. Maegdefessel, J. Heeren, L. Scheja, J. P. Bolaños, A. Rakovic, J. M. Spin, M. Stubbendorff, F. Ikeno, F. Länger, T. Zeller, L. Schulte-Uentrop, A. Stoehr, R. Itagaki, F. Haddad, T. Eschenhagen, S. Blankenberg, R. Kiefmann, H. Reichenspurner, J. Velden, C. Klein, A. Yeung, R. C. Robbins, P. S. Tsao and S. Schrepfer, *Nature*, 2014, **509**, 641.
30 P. W. Stacpoole and Y. J. Greene, *Diabetes Care*, 1992, **15**, 785.
31 A. Ф. GraloB and H. H. Mel'nikov, *Agrochem.*, 1985, **5**, 120.
32 (*a*) Z. Tong, P. G. Board and M. W. Anders, *Biochem. J.*, 1998, **331**, 371; (*b*) M. L. Hanson, P. K. Sibley, S. A. Mabury, D. C. G. Muir and K. R. Solomon, *Ecotoxicol. Environ. Saf.*, 2003, **55**, 46.
33 (*a*) D. A. V. W. Crabb, E. A. Yount and R. A. Harris, *Metabolism*, 1981, **30**, 1024; (*b*) D. Bahnemann, S. Kholuiskaya, R. Dillert, A. Kulak and A. Kokorin, *Appl. Catal., B*, 2002, **36**, 161.
34 (*a*) D. Rengstl, B. Kraus, M. Van Vorst, G. D. Elliott and W. Kunz, *Colloids Surf., B*, 2014, **123**, 575; (*b*) C. M. Williams, M. W. Couch, C. M. Thonoor and J. M. Midgley, *J. Pharm. Pharmacol.*, 1987, **39**, 153; (*c*) K. Amit, R. Vinoth, S. Snigdha, K. Prashant, K. Yogesh, S. Archana, M. Whelton, P. Vladimir, Poonam, G. Maria, G. Nikesh, K. Prakasha, D. Ravi, S. K. Brajendra, D. M. Ben and R. Brijesh, *Bioorg. Med. Chem.*, 2018, **26**, 3837; (*d*) J. Hulsbosch, D. E. De Vos, K. Binnemans and R. Ameloot, *ACS Sustainable Chem. Eng.*, 2016, **4**, 2917.
35 E. A. Baker, A. L. Hayes and R. C. Butler, *Pestic. Sci.*, 1992, **34**, 167.
36 M. Blesic, M. H. Marques, N. V. Plechkova, K. R. Seddon, L. P. N. Rebelo and A. Lopes, *Green Chem.*, 2007, **9**, 481.
37 Z. Z. Fan, W. Tong, Q. Zheng, Q. F. Lei and W. J. Fang, *J. Chem. Eng. Data*, 2013, **58**, 334.
38 D. Jordan, E. Tan and D. Hegh, *J. Surfactants Deterg.*, 2012, **15**, 587.
39 S. P. Stodghill, A. E. Smith and J. H. O'Haver, *Langmuir*, 2004, **20**, 11387.
40 E. Spielman-Sun, A. Avellan, G. D. Bland, R. V. Tappero, A. S. Acerbo, J. M. Unrine, J. P. Giraldo and G. V. Lowry, *Environ. Sci.: Nano*, 2019, **6**, 2508–2519.
41 M. W. Chase, *Am. J. Bot.*, 2004, **91**, 1645.
42 R. N. Malpassi, *Biocell*, 2006, **30**, 51.
43 P. Mayer and F. Reichenberg, *Environ. Toxicol. Chem.*, 2006, **25**, 2639.
44 D. Singh and M. Singh, *Weed Biol. Manage.*, 2008, **8**, 104.
45 T. Tind, T. J. Mathiesen, J. E. Jensen, C. Ritz and J. C. Streibig, *Pest Manage. Sci.*, 2009, **65**, 1257.
46 Z. G. Zhang, H. H. Wang and W. G. Shen, *J. Chem. Eng. Data*, 2013, **58**, 2326.
47 R. J. Strasser and A. Srivastava, *Photochem. Photobiol.*, 1995, **61**, 32.
48 G. Habibi and A. Vaziri, *Acta Agric. Slov.*, 2017, **109**, 393.
49 A. J. Strauss, G. H. J. Kruger, R. J. Strasser and P. D. R. Van, *Environ. Exp. Bot.*, 2006, **56**, 147.
50 M. González-ibarra, N. Farfán, C. Trejo, S. Uribe and B. Lotina-hennsen, *J. Agric. Food Chem.*, 2005, **53**, 3415.
51 Z. A. Huang, D. A. Jiang, Y. Yang, J. W. Sun and S. H. Jin, *Photosynthetica*, 2004, **42**, 357.
52 A. I. Vogel, B. S. Furniss, A. J. Hannaford, P. W. G. Smith and A. R. Tatchell, *Textbook of Practical Organic Chemistry*, Wiley John & Sons Inc, New York, 1989.